INT. J. REMOTE SENSING, 1993, VOL. 14, NO. 15, 2803–2818

Estimating the characteristics of vegetation canopies with airborne radar measurements

L. PREVOT†
INRA Station de Bioclimatologie, 78850 Thiverval-Grignon, France

M. DECHAMBRE, O. TACONET, D. VIDAL-MADJAR
CNET-CRPE, 10–12 Avenue de l'Europe, 78140 Vélizy, France

M. NORMAND and S. GALLE‡
CEMAGREF Division Hydrologie, BP121, 92185 Antony, France

(Received 4 February 1992, in final form 12 February 1993)

Abstract. Possible use of synthetic aperture radars (SAR) for monitoring agricultural canopies is investigated in this paper. Data have been acquired on the Orgeval watershed during the AGRISCATT'88 campaign. Four radar experiments were carried out with the airborne scatterometer ERASME (C and X bands, HH and VV polarizations, multi-incidence angles). Simultaneous ground measurements (soil moisture, leaf area index, water content of the canopy,...) were conducted on 11 wheat fields. Backscattering coefficients of the canopies are interpreted in the framework of semi-empirical 'water-cloud' models. A simple parametrization of the angular effect of soil roughness is introduced, allowing the simultaneous use of multi-incidence angle radar data. With a unique set of parameters for each radar configuration (frequency and polarization) the water-cloud model appears to describe adequately the backscattering of all the fields, over the range of incidence angles. It is shown that in this case, attenuation is the dominant effect of the vegetation and an inversion algorithm is proposed for estimating the water content of vegetation. This algorithm requires measurements at two different incidence angles and various combinations of radar configurations are then tested.

1. Introduction

With the recent launch of the European Remote Sensing Satellite ERS-1, several instruments operating in the microwave range are now available which can provide repetitive coverage of large areas in all weather conditions and independently of the time of the day. In particular, the imaging synthetic aperture radar operating at C-band (5·35 GHz), *VV* polarization and 23° incidence angle, although principally devoted to oceanographic applications, may also be a powerful tool for imaging land surfaces and for monitoring crops and water resources, as its spatial resolution is comparable to those of the optical sensors on board earth observation satellites (~20 m).

†Present address: INRA Station de Bioclimatologie, BP91, 84143 Montfavet, France.
‡Present address: ORSTOM Hydrologie, BP 5045, 34032 Montpellier, France.

Nevertheless, the interpretation of SAR images in terms of geophysical and biophysical parameters is neither as developed nor as straightforward as that of optical images and an important effort of modeling has to be made to understand scattering mechanisms that occur during the interaction between microwaves and vegetation canopies or bare soils. Methods already applied to the development of radar backscattering models from random media as soils or vegetation canopies can be divided in two general classes.

The first class involves theoretical and quite rigorous models, based on the resolution of the equations of electromagnetism, using a field approach (Fung and Ulaby 1978, Tsang and Kong 1981) or a radiative transfer method (Eom and Fung 1984, Ulaby *et al.* 1990). These models are useful for understanding volume scattering mechanisms, but unfortunately, they cannot be inverted and are computer-time consuming.

The second class deals with the so-called water-cloud semi-empirical models (Attema and Ulaby 1978), based on a first order solution of radiative transfer through a canopy, which use multiple regression analysis of the radar cross-section on soil and plants parameters. These models can be quite easily inverted, but experimental data are needed to adjust the parameters they involved.

These two approaches are quite different. The helpfulness to the understanding of volume scattering processes provided by theoretical models is obvious, but assumptions on vegetation characteristics (shape, size, orientation of the scatterers in the canopy,...) must be done, which may be not realistic. Furthermore, the numerous parameters included are more related to wave parameters than to vegetation characteristics. On the other hand, semi-empirical models are simple and well adapted to introduce experimental data and then to retrieve agricultural crop parameters. It is therefore very attractive to develop and use them as a framework for radar data inversion.

In this context, the European AGRISCATT'88 campaign held in 1988 and supported by ESA was devoted to applications of radar remote sensing over agricultural areas. Two airborne scatterometers flew over five European test sites, four times during the growing season. The aim of this campaign was firstly to build a database containing backscattering cross-sections and related ground data, acquired in 'natural conditions', (airborne radars over agricultural fields), and secondly to provide an experimental background for testing and developing algorithms for radar data inversion.

This paper is devoted to the main results concerning the estimation of agricultural crops parameters from the data acquired by the French scatterometer ERASME on the Orgeval watershed; the results dealing with hydrologic applications are presented in another paper (Normand *et al.* 1992).

In the subsequent sections, a brief description of the campaign is given; the main characteristics of ERASME and the geometry of measurements are given; contemporaneous ground measurements of soil and vegetation parameters are presented and the acquisition protocol is described. Canopy backscattering is then modelled using a semi-empirical water-cloud model. A simple parametrization of the angular effect of soil roughness is introduced, allowing the process of multi-incidence angle data. It is shown in that this case, the dominant effect of vegetation is an attenuation of the signal backscattered by the soil. An inversion algorithm, leading to the estimation of the vegetation water content, is then proposed and tested with different radar configurations.

2. Experiment

2.1. *The AGRISCATT'88 campaign on the French site*

The French test site is the *Orgeval* experimental watershed, located about 70 km East from Paris. Four experiments have been carried out, on the 16 and 30 June (days 168, 182) and the 12 and 28 July (days 194, 210). The scatterometer was performed along a 17 km flight axis, through the basin (see figure 1). A video camera was attached on the antenna support, looking in the same direction as the antennas. The time was added to the video image of the observed fields during the flights, so as to link together ERASME data and ground data acquired on each field.

2.2. *The scatterometer ERASME*

ERASME is a *C* and *X* band (5·35 and 9·65 GHz), FM-CW scatterometer of small size and low power, which can be easily installed in a small aircraft or an helicopter. It is designed as a research tool for the development of radar remote sensing in sea and land applications, as well as a calibration tool for ERS-1. It is a multi-incidence angle and one or two direct polarizations radar, whose main characteristics are summarized on table 1. A complete technical description of ERASME, in a previous mono-frequency version, can be found in Bernard *et al.* 1986.

During AGRISCATT'88, ERASME was operated for the first time in a forward looking mode as the quite large aperture of the antennas (see table 1) provides a large range of incidence angles. This allows the measurement of backscattering coefficients of a same target, viewed quasi instantaneously with different incidence angles, as it is shown on figure 2. The cross-track resolution is given by the antenna beamwidth and the along-track resolution is obtained by range discrimination. ERASME is a high range resolution (1 m) radar and the antenna footprint on the ground is about 20 m by 20 m, for a flying altitude of about 350 m. The radar

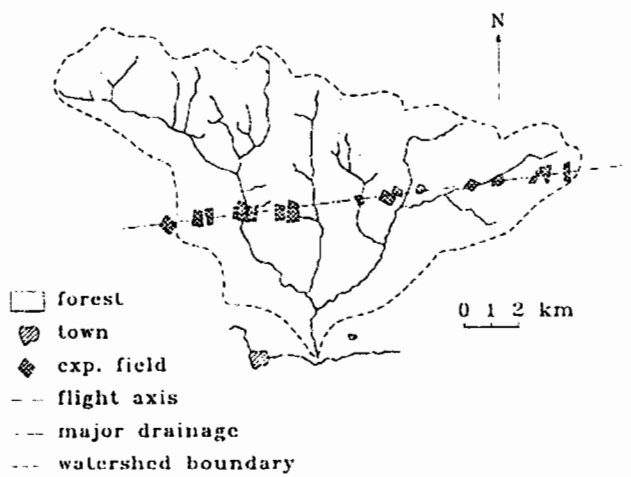

Figure 1. The flight line across the Oregeval basin.

Table 1. Characteristics of the ERASME scatterometer.

Type	Forward looking FM-CW
Central frequencies	5·35 GHz (*C*-band) and 9·65 GHz (*X*-band)
Transmitted power	11·2 dBm at *C*-band (13 mW) 20·0 dBm at *X*-band (100 mW)
Modulation	Sawtooth, 3 ms period
Bandwidth	220 MHz (1 m range resolution)
Transmitting antennas	*H* and *V* gain: 13 dB *C* and *X* aperture: ± 18·5 by ± 16
Receiving antennas	*C*-band *H*-polar gain: 23·2 dB, aperture: ± 8·5° by ± 1·8° *X*-band *V*-polar gain: 15·1 dB, aperture: ± 11·5 by ± 1·6 (apertures at 3 dB)
Altimeter antenna	Scalar horn, nadir-looking
Flight altitude	Nominal: 350 m
Internal calibration	Bulk acoustic device at *C*-band corresponding to a 300 *m* two-way travel line
'Pixel' size	approximately 20 m by 20 m
Signal processing	FFT analyser, 512 points, 3 ms synchronization waveform bandwidth: 100 kHz frequency resolution: 0·5 kHz local oscillator: 120 or 150 kHz
Acquisition	LSI 11/23, CCT tape recorder 8 analog lines for aircraft sensors (pitch, roll, ...)

configurations available during AGRISCATT'88 are summarized on table 2: during each experiment, two flights were performed along the same axis, one with a looking angle of 23° (the same incidence angle as for ERS-1) and the other one at 38°, allowing measurements with incidence angles respectively ranging from 15° to 30° and from 30° to 45°.

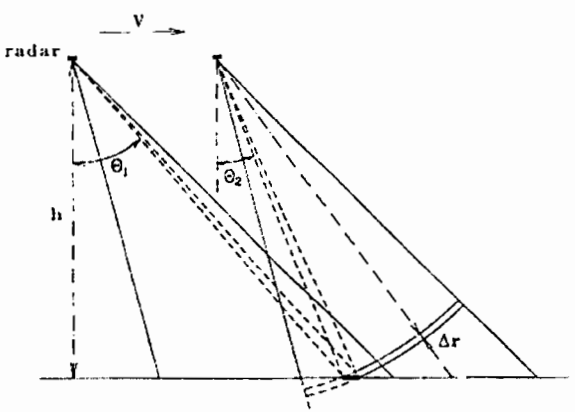

Figure 2. Geometry of ERASME forward-looking mode. A same target is first 'seen' at high incidence angle (θ_1), then at low incidence angle (θ_2). h is the flying altitude, Δr is the range resolution, V is the speed of the carrier.

Table 2. Radar configurations available during the AGRISCATT'88 campaign.

Frequency (wavelength)	Polarization	Incidence
C-band 5·35 GHz (5·6 cm)	*HH*	15° 20° 25° 30° (23°)
X-band 9·65 GHz (3·1 cm)	*VV*	30° 35° 40° 45° (38°)

External absolute calibration was carried out by flying ERASME over 3 corner reflectors, installed on an airport runway, close to the flight axis. The precision of ERASME measurements is computed using the radar budget equation. It is found to be better than 1 dB at the vicinity of the maximum of the antenna lobe, and to range between 1 and 2 dB at the edges. Thus, the only incidence angles used in this study are 20°, 25° and 35°, 40°.

2.3. *Ground measurements*

Along the flight axis, 11 wheat fields were selected for ground measurements, which are summarized on table 3, where the corresponding symbols are defined. As surface soil moisture can vary rapidly, soil moisture measurements were performed simultaneously with radar acquisition, whereas canopy measurements were carried out within the same week.

The gravimetric soil moisture in the upper layer (0–5 cm) was measured by using the gravimetric method. For each field, samples were taken every 50 m along the flight axis. Bulk density was determined by using a gamma-neutron probe, allowing to calculate the volumetric soil moisture (see Normand *et al.* 1992 for more details).

Vegetation height on the test fields was measured every 25 m along the flight axis. Three samples of 50 cm long by 3 rows (about 50 cm by 50 cm) were taken in each field and immediately put in airtight bags. They were weighted, giving the total fresh biomass, then dried in an oven, giving the total dry biomass and water content. Green leaf area index was measured with an optical planimeter. In addition, phenological stages were noted and the experiment covered the period between flowering and maturity. The temporal variations of the vegetation parameters during the campaign are plotted on figure 3, along with the evolution of surface soil moisture. One can see that the experiment provides a quite large range of values for these ground variables.

3. Backscattering model

3.1. *Description of the water-cloud model*

Water-cloud models are commonly used to interpret radar data in terms of soil and vegetation variables (Attema and Ulaby 1978, Mo *et al.* 1984, Paris 1986,

Table 3. Ground measurements, and corresponding symbols and units.

Soil	Surface moisture	m_s	$cm^3\ cm^{-3}$
Vegetation	Canopy height	h	m
	Green LAI	L	$m^2\ m^{-2}$
	Total water content	m_v	$kg\ m^{-2}$
	Dry biomass	M_s	$kg\ m^{-2}$
	Phenological stage		

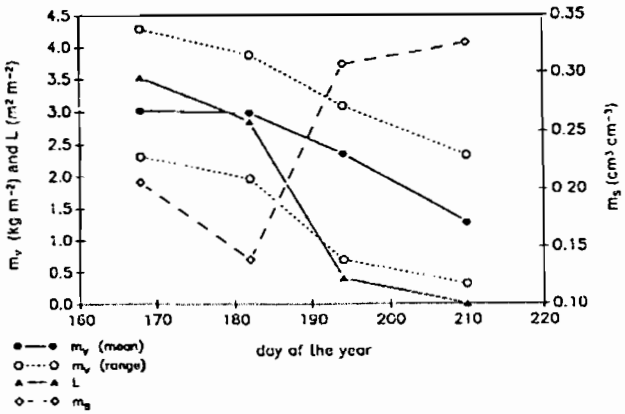

Figure 3. Temporal evolution of the main ground variables measured during the AGRISCATT'88 experiment: surface soil moisture: m_s, vegetation water content: m_v, green leaf area index: L. Each point is the average over the 11 wheat fields. The range of m_v values is also given.

Bernard *et al.* 1987, Bouman 1991): they involve bulk variables such as surface soil moisture and vegetation biomass (water content or leaf area index) and the number of parameters to fit is low. Thus they can easily be inverted if several radar configurations are available (Attema 1984, Prévot *et al.* 1988, Bouman 1991). As ERASME offers the great advantage to provide radar cross-sections measured at several frequencies, incidence angles and polarizations, we used water-cloud models to interpret its data.

Let us first briefly recall the basic assumptions set in water-cloud models (Attema and Ulaby 1978):

(*a*) The vegetation is represented as a homogeneous horizontal cloud of identical water spheres, uniformly distributed throughout the space defined by the soil surface and the vegetation height.
(*b*) Only single scattering is considered.
(*c*) The only significant variables are the height of the canopy layer and the cloud density, the latter assumed to be proportional to the volumetric water content of the canopy.

Under these assumptions, the radar cross-section of the canopy σ° is expressed as the incoherent sum of the contribution of the vegetation layer σ°_{veg} and the contribution of the soil σ°_{soil}, the latter being attenuated through the vegetation. For an incidence angle θ, we can write:

$$\text{Whole canopy:} \quad \sigma^\circ = \sigma^\circ_{veg} + \tau^2 \sigma^\circ_{soil} \tag{1}$$

$$\text{Vegetation:} \quad \sigma^\circ_{veg} = A \cos\theta (1 - \tau^2) \tag{2}$$

$$\tau^2 = \exp(-2Bm_v/\cos\theta) \tag{3}$$

where the different backscattering coefficients σ° are expressed in power units, τ^2 is the two-way attenuation through the vegetation, and m_v is the water content of the canopy (kg m^{-2}), which is equal to the product of the volumetric water content times the height of the canopy.

For a given radar configuration, the soil contribution is usually expressed as a linear function of its surface moisture content m_s (Ulaby *et al.* 1978, Bernard *et al.* 1986, Bruckler *et al.* 1988):

$$\sigma^\circ_{soil} = C + Dm_s \tag{4}$$

where σ°_{soil} is expressed in dB.

Here, the vegetation is characterized by its water content m_v (kg m^{-2}) and the soil by the volumetric water content m_s (cm^3 cm^{-3}) of its surface. Only four parameters are needed, A and B for the vegetation and C and D for the soil. The parameter A corresponds to the albedo of the vegetation and B is an attenuation factor. The parameter D is the sensitivity of the signal to soil moisture and C can be considered as a calibration constant. These four parameters have to be fitted for each radar configuration.

3.2. *A simple parametrization of the angular effect of soil roughness*

Soil surface roughness greatly affects microwave backscattering and therefore acts as a disturbing factor for soil moisture or biomass estimations. For soil moisture estimation, this effect can be minimized by using incidence angles ranging from 7° to 17° (Ulaby *et al.* 1978, Jackson and O'Neill 1985), but this configuration is not available for ERS-1, as well as for the future spaceborne platforms, because it does not provide a sufficiently high spatial resolution. It is therefore necessary to account for soil roughness effects, which can be interpreted as angular effects, the backscattering coefficients having angular variations all the more important as the soil roughness is small.

Moreover, when the density of vegetation increases volume scattering cannot be neglected and its angular effects are quite similar to those induced by an increasing soil roughness, which could be confusing. Finally, as multi-angular configurations are needed to estimate the biomass of vegetation canopy by means of radar remote sensing (Attema 1984, Prévot *et al.* 1988, Bouman 1991), a parametrization of the roughness effects must be included in canopy backscattering models.

In the case of the water-cloud model, the parametrization of roughness effects must keep the model as simple as possible, because one of the advantages of this model is that it can be easily handled. Let us introduce this angular effect in the cloud model as follows, keeping in mind the previous remarks. Several theoretical (Autret *et al.* 1989) or experimental (Ulaby *et al.* 1978) studies have shown that for frequencies greater than 4 GHz, the sensitivity parameter D in (4) could be assumed to be constant in a first approximation. The more important dependence of (4) with the radar configuration and the soil roughness leaves in the parameter C. The variations of C with the incidence angle may be linearized for angles ranging from 20° to 40°. This linearization represents an averaged behaviour of the radar cross-section in terms of roughness effects, and we propose to rewrite (4) in the following form:

$$\sigma^\circ_{soil} = C(F, \theta) + Dm_s \tag{5}$$

with

$$C(F, \theta) = C_1(F) - \theta C_2(F) \tag{6}$$

where F denotes the radar configuration (frequency and polarization).

This parametrization considers the effect of soil moisture (dielectric properties) and the effect of roughness (geometry of the surface) as independent, as shown by Bertuzzi *et al.* (1992). It adds only little complexity to the initial water-cloud model, assuming that if D is a constant, there are still only four parameters to be fitted. The parameter C_1 can be considered as a calibration constant (dB), as C_2 is the angular sensitivity of the soil signal (dB^{-1}), which is related to roughness. The sensitivity to soil moisture D has to be determined using a radar configuration for which the signal is the less sensitive as possible to the vegetation. The determination of the parameters C_1 and C_2 requires data acquired at several incidence angles, for each radar configuration (frequency and polarization).

3.3. *Fitting of the model*

Previous experimental studies (Ulaby *et al.* 1978, 1979, Le Toan and Pausader 1981, Jackson and O'Neill 1985) have shown that the best radar configurations for soil moisture estimation are defined by a low frequency ($\leqslant 5$ GHz), low incidence angle ($\sim 14°$) and *HH* polarization. Therefore, the best available ERASME configuration for determining D is *C*-band, 20°, and *HH* polarization. The parameters A, B, C, and D of the initial model (soil contribution represented by (4)) are simultaneously determined in this configuration, using a nonlinear least squares regression algorithm. The parameter D is found to be equal to 0·304 (dB(cm^{-3}cm^{+3})), which compares well to results obtained in other studies (Bruckler *et al.* 1988).

The parameter D is then assumed to be constant, and the parameters A, B, C_1 and C_2 of the modified model (soil contribution represented by (5) and (6)) are fitted on the radar cross-sections measured at 20° and 40°, for *C*-band, *HH* polarization and for *X*-band, *VV* polarization, using the same algorithm. Figure 4 shows the results of the complete model calibration, and the values of the four parameters are given in table 4.

For both configurations, the model can represent the data for a large range of backscattering coefficients. No bias is observed and the dispersion of the data is rather low if one considers that they come from 11 different fields. In fact, the residual sums of squares are equal to 1·1 dB for both configurations, which is of the same magnitude as the precision scatterometer.

The shape of the model is plotted as a function of the ground variables m_s and m_v on figure 5 (*C*-band, *HH* polarization) and on figure 6 (X-band, *VV* polarization). We can see that in *C*-band, the contribution of the vegetation to the backscattered signal, denoted σ°_{veg}, is not significantly different from zero, as $A = 0$. The attenuation, represented by the parameter B, is weak, even if not at all negligible. As expected, the attenuation in *X*-band is important, and for high values of the biomass ($m_v \geqslant 3{\cdot}5\,\mathrm{kg\,m^{-2}}$) the contribution of the vegetation σ°_{veg} is dominant in (1). The values of the attenuation parameter B obtained here are in good agreement with those obtained in similar studies reviewed by Jackson and Schmugge (1991).

For each radar configuration, a unique value of the 'roughness' parameter C_2 seems good enough to represent the different fields observed. This corresponds to the implicit hypothesis that the roughness was almost constant during the experiment and throughout the fields and this is likely to be verified as all the fields were cultivated with similar tillage techniques, and at a time of the year when the weather had homogenized the roughness of the soil surface.

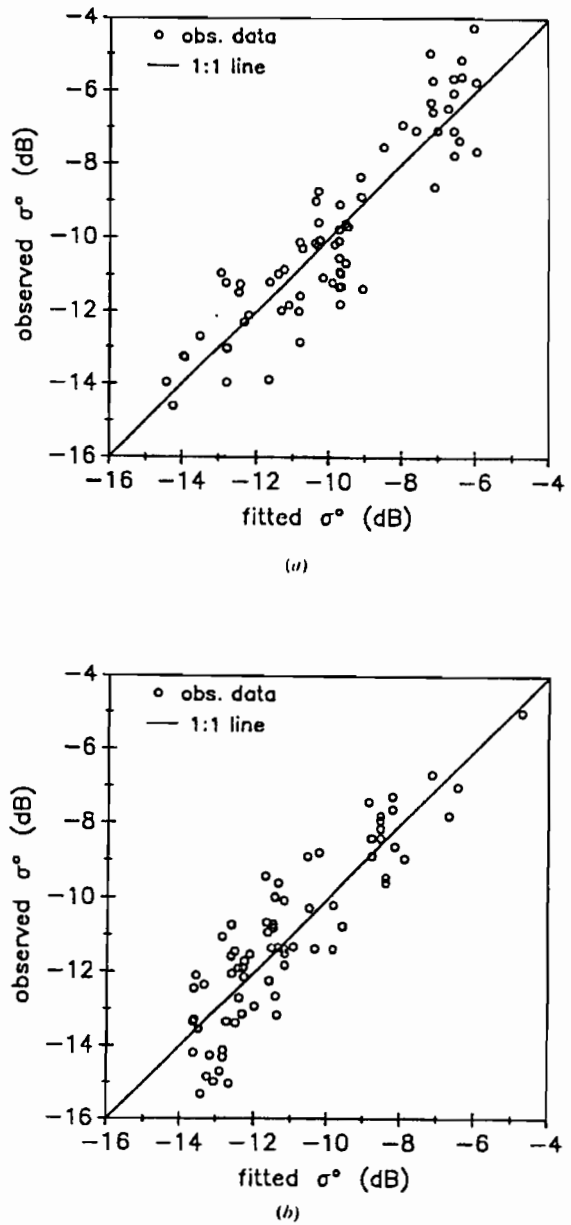

Figure 4. Calibration of the model, using data acquired at 20° and 40°: measured radar cross-sections versus fitted radar cross-sections. Each point correspond to a field (*a*): *C*-band, *HH* polarization, (*b*): *X*-band, *VV*-polarization.

Table 4. Model calibration: values of the fitted parameters (the parameter $D = 0{\cdot}304$ is assumed to be constant). R^2: square of the correlation coefficient, *std*: standard error of residuals.

	A	B	C_1	C_2	R^2	std
C-HH	0·000	0·086	−13·4	0·155	0·82	1·1
X-VV	0·056	0·423	−11·2	0·153	0·78	1·1

The validity of the model is verified by using the data acquired at 25° and 35° and the results are plotted on figure 7. The slopes of the lines corresponding to the linear regression of the measured radar cross-sections against the predicted radar cross sections are not significantly different from 1. The standard deviations of the residuals are respectively 1·13 dB for *C*-band and 1·08 dB for X-band, which still compares well with the precision of ERASME.

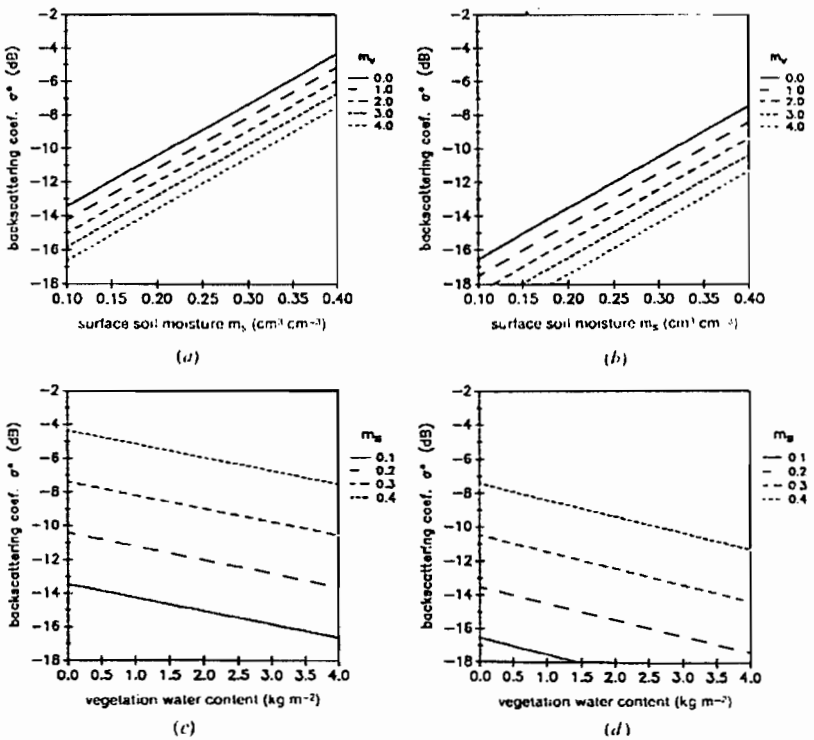

Figure 5. Shape of the model in *C*-band. The model is plotted as a function of the soil moisture m_s, for different values of the vegetation water content m_v (*a* and *c*), and as a function of m_v for different values of m_s (*b* and *d*), for two radar configurations: *C-HH*-20° (*a* and *b*) and *X-HH*-40° (*c* and *d*).

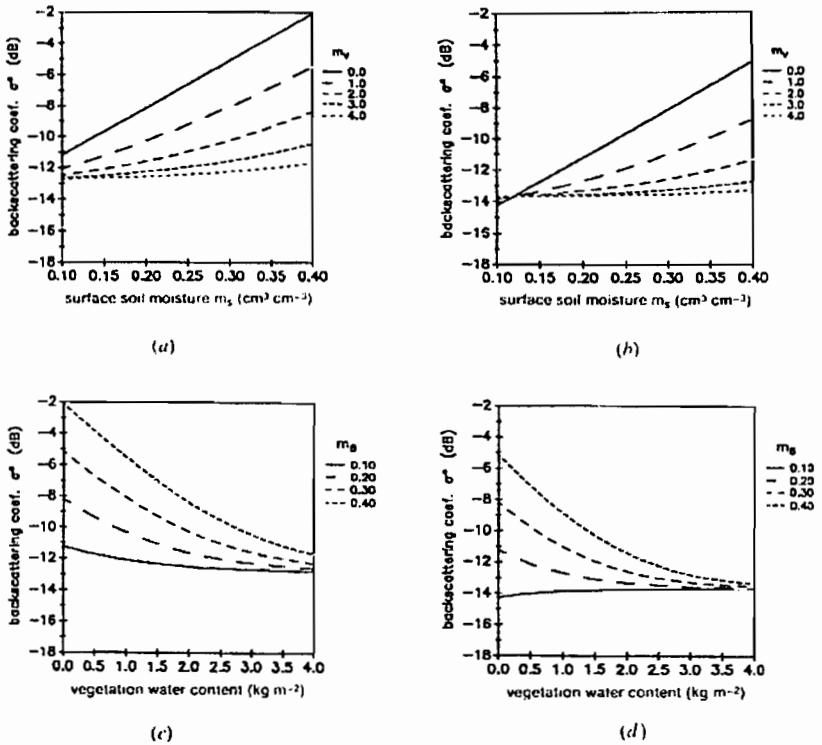

Figure 6. Shape of the model in *X*-band. Same legend as figure 6 with: *X-HH*-20° (*a* and *b*) and *X-HH*-40° (*c* and *d*).

4. Inversion of the model and vegetation water content estimation

The model presented in the previous paragraph is valid for a large range of incidence angles and ground variables. Furthermore, a unique set of parameters can adequately represent the behaviour of 11 different fields, covered with the same type of vegetation. It is therefore tempting to use it as an inversion algorithm of radar data. As can be seen in figures 5 and 6, the effect of the vegetation is mainly an attenuation of the signal returned by the underlying soil. By neglecting the contribution of the vegetation, the model can be simplified in the following form:

$$\sigma^\circ = \exp(-2Bm_v/\cos\theta)\sigma^\circ_{soil} \tag{7}$$

where σ°_{soil} is given by (5) and (6).

When expressed in dB units, this expression leads to a linear function of the surface variables m_s and m_v:

$$\sigma = B'm_v/\cos\theta + C + Dm_s \tag{8}$$

where $C = C_1 + C_2\theta$ and $B' = 10B/\ln 10$ depends on the radar configuration (frequency and polarization).

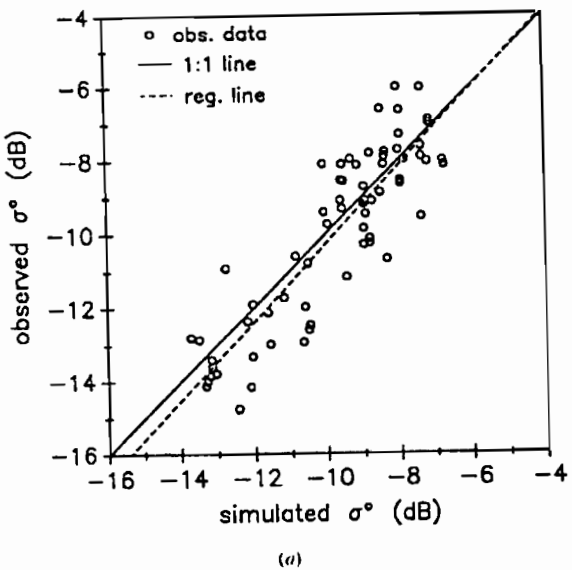

(a)

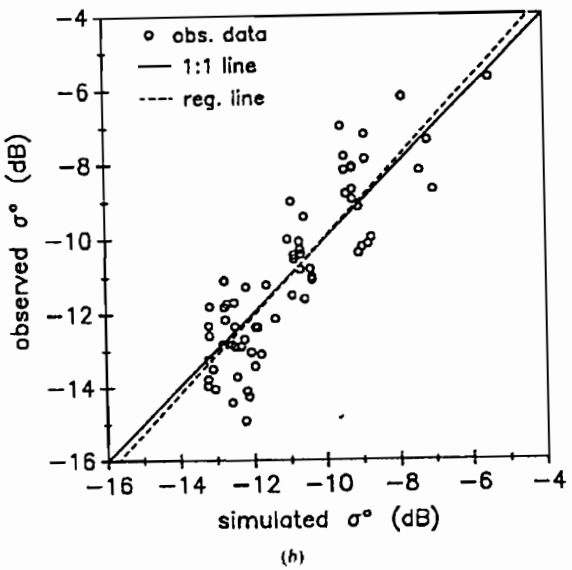

(b)

Figure 7. Validation of the model, using data acquired at 25° and 35°: measured radar cross-sections versus simulated radar cross-sections. Each point correspond to a field. (*a*): *C*-band, *HH* polarization, (*b*): *X*-band, *VV*- polarization.

The advantage of this simplified formulation is that it can be analytically inversed. Indeed, if one can dispose of measurements acquired with two different radar configurations, denoted *a* and *b*, the following system can be solved in m_r:

$$\sigma^\circ_a = B'_a m_r/\cos\theta_a + C_a + Dm_s$$
$$\sigma^\circ_b = B'_b m_r/\cos\theta_b + C_b + Dm_s \qquad (9)$$

which gives an estimate of the vegetation water content m_r independently from the surface soil moisture m_s.

Keeping in mind that this method of inversion relies on the difference of attenuation by the vegetation between two radar configurations, it has been tested on the different pairs of configurations available during AGRISCATT'88 (see table 5). Figure 8 presents the results of the inversion for the two pairs giving the better results: *C-HH*-20°/40° and *X-VV*-20°/40°. The inversion algorithm is unbiased since in both cases the regression lines do not differ significantly from the 1:1 line.

However, the data exhibit some scatter around the regression line. This is not surprising as a single simple model is used to represent 11 fields covered with different varieties and having different surface roughness. Taking that into account, the accuracy of the inversion algorithm, expressed in table 6 by the residual standard deviations of the estimated canopy water content, is satisfactory.

More scatter of the data is observed in *C*-band than in *X*-band (see figure 8 and table 6). As the quality of the fitting of the direct models in both frequencies was similar (see figures 4 and 7, table 4), it can be concluded that the difference comes from their ability to be inverted. The similar attenuation by the vegetation in *C*-band leads to less difference in attenuation between 20° and 40° and therefore less accuracy in the inverison algorithm. For wheat canopies, *C*-band appears not to be sensitive enough to vegetation effects to provide an accuracy compatible with agronomic applications.

Table 5 shows that only multi-angular configurations can be used with this method and that multi-frequency configurations do not seem to increase the accuracy of the inversion. This is probably due to the fact that the scattering mechanisms are not well modelled with such a simple model when going from *C*-band to *X*-band. Nevertheless, it is important to notice that, if the *X*-band with two incidence angles appears to be good enough to estimate vegetation biomass, only *C*-band, or a lower frequency, is able to give significant information on soil moisture (Ulaby *et al.* 1979, Jackson and Schmugge 1991). Finally, let us remember that the inversion method presented here can be used only when the vegetation is not so dense (for example, when leaf area index is less than 3).

Table 5. Estimation of the canopy water content by inversion: residual standard deviations (in kg m^{-2}) for different pairs of radar configurations.

	C HH 20	*C HH* 40	*X VV* 20
X VV 40	0·75	1·29	**0·49**
X VV 20	1·18	2·01	
C HH 40	**0·62**		

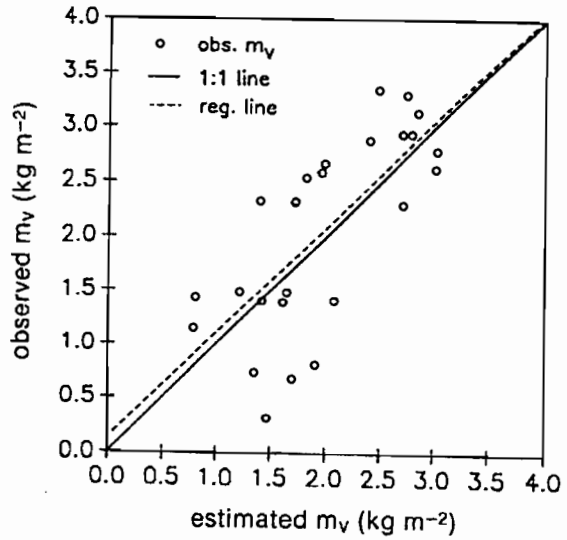

(*a*)

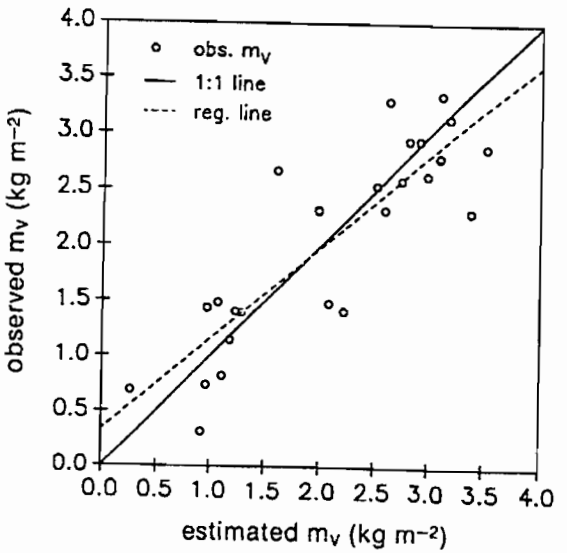

(*b*)

Figure 8. Estimation of the vegetation water content m_v by inversion of the model, for the two best radar configurations: (*a*): *C-HH*-20° and *C-HH*-40°, (*b*): *X-VV*-20° and *X-VV*-40°. The coefficients of the regression lines are given in table 5.

Table 6. Estimation of the canopy water content by inversion: coefficients of the regression lines in figure 8.

configuration	slope	std	intercept	std	R^2	ddl
C-HH-20°/40°	0·975	0·193	0·132	0·635	0·515	24
X-VV-20°/40°	0·822	0·100	0·339	0·465	0·739	24

5. Conclusion

Devoted to the study of radar signature of agricultural areas and carried out in 'natural conditions', i.e., airborne scatterometer data and agricultural fields, the AGRISCATT'88 experiment demonstrates the capability of active microwave techniques for crop monitoring, providing several simultaneous radar configurations are available. As the operational use of radar remote sensing requires the development of appropriate inversion schemes, two algorithms have been introduced and tested in this paper.

A simple parametrization of the angular effect of soil roughness was first introduced. Its degree of complexity was comparable to those of the water-cloud model, adding only one parameter. This parametrization permitted the simulation of radar cross-section over a large range of incidence angles (20° to 40°), thus leading to the interpretation of multi-incidence data sets. A simple method for the estimation of the vegetation water content was then developed and tested, giving satisfactory results. This method can be used when the canopy contains sparse scatterers, i.e., for low levels of biomass, and requires radar data acquired at two sufficiently different incidence angles, typically 20° and 40°.

The ability of water-cloud models to simulate radar cross-sections of crop canopies is all the more corroborated here, as a unique set of parameters was sufficient to describe globally the backscattering behaviour of several wheat fields. Nevertheless, both algorithms developed here need further testing. The parametrization of roughness effect should be tested against more detailed data sets or against theoretical models of surface scattering. The inversion method should be tried out on other types of canopies.

The inversion algorithm has been tested with different pairs of radar configurations, leading to the conclusion that *X*-band with two incidence angles provided a good enough estimation of vegetation water content. As previously pointed out, only a lower frequency, as *L* or *C* bands, can give significant information on soil surface moisture. Furthermore, it is likely that the results presented here were made partly possible by a rather constant soil roughness over the different fields observed. A dual-frequency, dual-incidence angle radar system would probably be the only way to achieve inversion when the roughness is varying.

Acknowledgments

This study was supported by ESA in the framework of the Earth Observation Preparatory Program and by the French National Program for Remote Sensing. The authors wish to express their gratitude to their colleagues from CEMAGREF, CNET and INRA for the help during the experiments.

References

ATTEMA, E., 1984, Radar scattering models for vegetation canopies. In *Proceedings of the 2nd Symposium on Spectral Signatures of Objects in Remote sensing*. (Bordeaux), INRA-CNES-ISPRS, Les colloques de l'INRA, pp. 577–587.

ATTEMA, E., and ULABY, F., 1978, Vegetation modeled as a water cloud. *Radio Science*, **13**, 357–364.

AUTRET, M., BERNARD, R., and VIDAL-MADJAR, D., 1989, Theoretical study of the sensitivity of the microwave backscattering coefficient to the soil surface parameters. *International Journal of Remote Sensing*, **10**, 171–179.

BERNARD, R., VIDAL-MADJAR, D., BAUDIN, F., and LAURENT, G., 1986, Data processing and calibration for an airborne scatterometer. *I.E.E.E. Transactions on Geoscience and Remote Sensing*, **24**, 707–716.

BERNARD, R., FREZEL, M., VIDAL-MADJAR, D., GUYON, D., and RIOM, J., 1987, Nadir looking airborne radar and possible applications to forestry. *Remote Sensing of Environment*, **21**, 297–309.

BERTUZZI, P., CHANZY, A., VIDAL-MADJAR, D., and AUTRET, M., 1992, The use of a microwave backscatter model for retrieving soil moisture over bare soil. *International Journal of Remote Sensing*, **13**, 2653–2668.

BOUMAN, B., 1991, Crop parameter estimation from ground-based X-band (3-cm wave) radar backscattering data. *Remote Sensing of Environment*, **37**, 193–205.

BRUCKLER, L., WITONO, H., and STENGEL, P., 1988, Near surface soil moisture estimation from microwave measurements. *Remote Sensing of Environment*, **26**, 101–121.

EOM, H., and FUNG, A., 1984, A scatter model for vegetation up to Ku-band. *Remote Sensing of Environment*, **15**, 185–200.

FUNG, A., and ULABY, F., 1978, A scatter model for leafy vegetation. *I.E.E.E. Transactions on Geoscience and Remote Sensing*, **GE-16**, 281–286.

JACKSON, T., and O'Neill, P., 1985, Aircraft scatterometer observations of soil moisture on rangeland watersheds. *International Journal of Remote Sensing*, **6**, 1135–1152.

JACKSON, T., and SCHMUGGE, T., 1991, Vegetation effects on the microwave emission of soils. *Remote Sensing of Environment*, **36**, 203–212.

LE TOAN, T., and PAUSADER, M., 1981, Humidité du sol et rétrodiffusion radar: expériences dans la région 1·5–9·0 GHz. In *Proceedings of the Spectral Signature of Objects in Remote Sensing Symposium* (Avignon), Les colloques de l'INRA, pp. 303–318.

MO, T., SCHMUGGE, T., and JACKSON, T., 1984, Calculations of radar backscattering coefficient of vegetation-covered soils. *Remote Sensing of Environment*, **15**, 119–133.

NORMAND, M., GALLE, S., BENALLEGUE, M., DECHAMBRE, M., TACONET, O., VIDAL-MADJAR, D., and PRÉVOT, L., 1992, Soil moisture assessment at a basin scale using active microwave remote sensing: the Agriscatt'88 airborne campaign on the Orgeval watershed. To be submitted to *International Journal of Remote Sensing*.

PARIS, J., 1986, The effect of leaf size on the microwave backscattering by corn. *Remote Sensing of Environment*, **19**, 81–95.

PRÉVOT, L., CHAMPION, I., and GUYOT, G., 1988, Extraction de caractéristiques du sol et de la végétation à partir de données de télédétection hyperfréquences. In *Proceedings of the 4th International Colloquium-Spectral Signatures in Remote Sensing* (Aussois), CNES-INRA-ESA-CNRS, ESA SP-287, pp. 7–12.

TSANG, L., and KONG, J., 1981, Applications of strong fluctuation random medium theory to scattering from vegetation-like half space. *I.E.E.E. Transactions on Geoscience and Remote Sensing*, **GE-19**, 62–69.

ULABY, F., BATLIVALA, P., and DOBSON, M., 1978, Microwave backscatter dependence on surface roughness, soil moisture and soil texture: Part I—bare soil. *I.E.E.E. Transactions on Geoscience Electronics*, **GE-16**, 286–295.

ULABY, F., BRADLEY, G., and DOBSON, M., 1979, Microwave backscatter dependence on surface roughness, soil moisture and soil texture: Part II—vegetation covered soil. *I.E.E.E. Transactions on Geoscience Electronics*, **GE-17**, 33–40.

ULABY, F., SARABANDI, K., MCDONALD, K., WHITT, M., and DOBSON, M., 1990, Michigan microwave canopy scattering model. *International Journal of Remote Sensing*, **11**, 1223–1253.